# Carbon Nanotubes as Free-Radical Scavengers

## Annia Galano\*

Departamento de Química, Universidad Autónoma Metropolitana-Iztapalapa, San Rafael Atlixco 186, Col. Vicentina, Iztapalapa, C. P. 09340, México D.F., México, and Instituto Mexicano del Petróleo, Eje Central Lázaro Cárdenas 152, 07730, México D.F., México

Received: February 15, 2008; Revised Manuscript Received: March 26, 2008

Density functional theory calculations have been used to model the potential ability of single-walled carbon nanotubes (SWCNT) to act as free-radical scavengers. The reactions of a (5,5) SWCNT fragment with six different radicals have been studied, and for hydroxyl radical, which is the most reactive and dangerous from all of the studied set, up to four additions were modeled. Energetic considerations show that, once a first radical is attached to the nanotube, further additions are increasingly feasible, suggesting that SWCNTs can act as free-radical sponges. For reactions with OH radicals, subsequent additions are expected to lead to products where the OHs are distributed in groups rather than regularly spread on the nanotube. Because nanotubes with none or an even number of OH groups attached are stable (nonradical) species that can be used for other purposes, their properties were analyzed in terms of global reactivity indexes and density of states (DOS). The results from these analyses suggest that, by controlling the proportion of OH on the nanotubes, their properties can be manipulated.

#### Introduction

Since their discovery, 1 carbon nanotubes (CNTs) have attracted a great deal of attention worldwide. This interest is based on their unique physical and chemical properties that could impact broad areas of science and technology.<sup>2</sup> These properties are related to their peculiar structure. CNTs are cylindrical molecules composed of carbon atoms that can be thought of as rolled-up graphene sheets. Accordingly, these large arrays of conjugated double bonds are expected to show great electron donor and acceptor capabilities; that is, these structures can easily cope with lack or excess of electrons. In a similar way, fullerenes are often referred to as electron sponges.<sup>3,4</sup> On the other hand, other compounds with long conjugated C=C chains, such as carotenoids, have been found to be excellent free-radical scavengers.<sup>6,5</sup> Thus, the next logical question is whether CNTs can also be used as free-radical traps. This would be a very useful application of CNTs because free radicals are known to be highly damaging species in very diverse systems, such as the atmosphere and living organisms. A very recent study has indicated that purified multiwalled CNTs are very effective scavengers of radical oxygenated species.<sup>7</sup> In addition, several studies on the ability of fullerenes<sup>8–10</sup> and graphite<sup>11,12</sup> to easily react with free radicals have also been reported.

Reactions between CNTs and free radicals can be thought of in terms of two different mechanisms: electron-transfer (ET) processes and adduct formation. In addition to the very desirable function of breaking free-radical chain reactions, the second mechanism is also of interest for wall functionalization of CNTs. Indeed, it has recently been shown that this grafting process has some advantages over the ionic approach.<sup>13</sup> Accordingly, it is the aim of this work to focus on the addition mechanism. A finite fragment of (5,5) armchair single-walled CNT (SWCNT) and a series of six different radicals were used for this purpose.

The studied systems were modeled using density functional theory (DFT), which has been successfully applied to predict

many properties of ground-state systems with high accuracy and with less computational effort than some of the traditional ab initio methods. This important feature has made DFT successful in the study of different problems involving large systems. <sup>14</sup> The study of different reactivity parameters within the DFT framework has been widely used to describe the chemical reactivity of atoms, molecules, clusters, and solids. <sup>15</sup>

### **Computational Details**

Electronic structure calculations were performed with the Gaussian 03<sup>16</sup> program. Full geometry optimizations and frequency calculations were carried out for all stationary points using the B3LYP hybrid Hartree-Fock density functional and the 3-21G basis set. The energies of all of the stationary points were improved by single-point calculations at the B3LYP/6-31G(d,p) level of theory. Thermodynamic corrections at 298 K were included in the calculation of relative energies. Spinrestricted calculations were used for closed-shell systems, and unrestricted calculations were used for open-shell systems. Local minima and transition states were identified by the number of imaginary frequencies (NIMAG = 0 and 1, respectively). In addition, the vibrational modes with imaginary frequencies were inspected using the GaussView<sup>17</sup> program, and it was confirmed that they corresponded to the proper transition vector. In addition, it is our opinion that any theoretical model intended for practical applications must be analyzed in terms of Gibbs free energies; this implies the necessity of performing frequency calculations, which are particularly computationally expensive. Accordingly, it seems a better compromise to perform frequency calculations at a low level of theory than to increase the level of theory and analyze the results only in terms of electronic energy.

The stationary points were first modeled in the gas phase (vacuum), and solvent effects were included a posteriori by single-point calculations using the polarizable continuum model, specifically the integral—equation—formalism (IEF-PCM)<sup>18</sup> at the B3LYP/6-31G(d,p) level of theory, with benzene as the

<sup>\*</sup> Corresponding author. E-mail: agalano@prodigy.net.mx.

TABLE 1: Gibbs Free Energies of Reaction ( $\Delta G$ ) and Barriers ( $\Delta G^{\pm}$ ) at 298.15 K for the OH + Benzene **Gas-Phase Reaction** 

	$\Delta G^{\pm}$ (kcal/mol)	$\Delta G$ (kcal/mol)
B3LYP/6-31G(d,p)//B3LYP/3-21G	7.45	-7.04
B3LYP/6-311++G(d,p)	7.55	-4.47
CBS-QB3	8.88	-9.30

solvent to mimic nonpolar environments. Polar environments were not included because pure carbon nanotubes are not expected to be soluble in such medium. For all of the PCM calculations the solvent cavity was constructed using the UAHF atomic radii.

The accuracy of the level of theory used in the present work has been tested for a much smaller, but chemically similar reaction: OH + benzene, in the gas phase. For that purpose the results at the B3LYP/6-31G(d,p)//B3LYP/3-21G level were compared with those obtained at the B3LYP/6-311++G(d,p)and CBS-QB3 levels of theory (Table 1). According to the results in this table, the Gibbs free energies of reaction obtained at the B3LYP/6-31G(d,p)//B3LYP/3-21G level are between those obtained using B3LYP/6-311++G(d,p) and CBS-QB3. In addition, the discrepancies with the highest tested level (CBS-QB3) are about 1.3 and 2.3 kcal/mol for the barrier and the energy of reaction, respectively. These differences are lower than the mean absolute deviations from experimental data, which are estimated to be 3.29 and 4.37 kcal/mol for B3LYP using the G2/97<sup>19,20</sup> and G3/99<sup>21</sup> test sets, respectively. Accordingly, the expected accuracy of the results obtained using a modest basis set for geometry optimizations and frequency calculations is good enough to make reliable predictions, at least semiquantitatively.

#### **Results and Discussion**

The reactions of six different radicals with a CNT fragment have been studied. The CNT fragment was modeled as a finite (5,5) armchair nanotube, with the dangling bonds at the ends of the nanotube saturated by hydrogen atoms to avoid unwanted distortions. The length of the modeled fragment is equivalent to three hexagons, or about 8 Å. The sites of reaction were chosen as the central hexagons in all cases. The studied radicals (R) are hydroxyl, HO<sup>•</sup>; hydrogen peroxyl, HOO<sup>•</sup>; methyl, <sup>•</sup>CH<sub>3</sub>; methoxyl, CH<sub>3</sub>O<sup>•</sup>; methyl peroxyl, CH<sub>3</sub>OO<sup>•</sup>; and formyl, <sup>•</sup>CHO. In addition, for the OH radical, subsequent addition reactions were modeled, for up to four OH groups, and different relative positions of the trapped radicals were analyzed. For the formation of the first adduct, that involving only one free radical, the most relevant geometrical parameter that changes as the reaction progresses is the distance  $R \cdots C$  corresponding to the forming bond. These distances are reported for transition-state and product structures in Table 2. The enthalpies of reaction ( $\Delta H$ ) at room temperature for the radical additions to the CNT (5,5) fragment are also reported in Table 2. All of the studied reactions were found to be exothermic, with the exception of that invoving R=CH<sub>3</sub>OO in the gas phase. The order of exothermicity did not seem to be affected by the presence of a nonpolar solvent, and it was found to be  $OH > CH_3 > CHO > CH_3O > OOH > CH_3OO$ .

The Gibbs free energies of reaction ( $\Delta G$ ) and barriers ( $\Delta G^{\pm}$ ) at 298.15 K for all of the studied channels are reported in Table 3. For the gas phase, the calculations were performed using a standard state of 1 atm, as calculated from the Gaussian program outputs. However, for reactions in solution, the reference state was changed from 1 atm to 1 M, and solvent cage effects were

**TABLE 2: Distances of the Forming (Formed) Bond in** Transition States (Products) and Enthalpies of Reaction  $(\Delta H)$  at 298.15 K

radical	$\frac{R \cdots C \text{ bond } (\mathring{A})}{TS}$	product	$\Delta H_{\rm gas}$ (kcal/mol)	$\Delta H_{\rm sol}$ (kcal/mol)
ОН	d(O-C) = 2.32	1.48	-26.30	-29.30
OOH	d(O-C) = 1.99	1.52	-2.15	-6.23
$CH_3$	d(C-C) = 2.41	1.56	-18.97	-25.33
$CH_3O$	d(O-C) = 2.10	1.48	-10.28	-16.35
$CH_3OO$	d(O-C) = 1.98	1.51	0.60	-4.00
CHO	d(C-C) = 2.44	1.56	-11.88	-19.22

TABLE 3: Gibbs Free Energies of Reaction ( $\Delta G$ ) and Barriers ( $\Delta G^{\pm}$ ) and Rate Constants per Addition Site at 298.15 K

	$\Delta G_{ m gas}^{\pm}$ (kcal/mol)	$\Delta G_{ m gas}$ (kcal/mol)	$\Delta G_{ m sol}^{ m FV,\pm}$ (kcal/mol)	$\Delta G_{ m sol}^{ m FV}$ (kcal/mol)	$k_{\text{app-sol}}$ (L mol <sup>-1</sup> s <sup>-1</sup> )
ОН	9.22	-15.92	1.43	-23.35	$9.99 \times 10^{9}$
OOH	18.35	10.04	9.04	1.54	$3.59 \times 10^{7}$
$CH_3$	19.63	-7.17	3.94	-17.96	$9.52 \times 10^{9}$
$CH_3O$	15.81	2.22	4.03	-8.28	$9.44 \times 10^{9}$
CH <sub>3</sub> OO CHO	22.15 11.18	13.22 0.05	10.33 4.79	4.18 $-11.71$	$4.07 \times 10^6$ $8.24 \times 10^9$

included according to the corrections proposed by Okuno,<sup>22</sup> taking into account the free volume (FV) theory.23 These corrections are in good agreement with those independently obtained by Ardura et al.<sup>24</sup> and have been successfully used by other authors.<sup>25</sup> The expression used to correct the Gibbs free energy is

$$\Delta G_{\text{sol}}^{\text{FV}} \approx \Delta G_{\text{sol}} - RT \{ \ln[n \times 10^{(2n-2)}] - (n-1) \}$$
 (1)

where nrepresents the total number of reactant moles. According to eq 1, the cage effects in solution cause  $\Delta G$  to decrease by 2.54 kcal/mol for bimolecular reactions at 298 K. This lowering is expected because the cage effects of the solvent reduce the entropy loss associated with any addition reaction or transition-state formation in reactions with molecularity equal to or greater than 2. Therefore, if the translational degrees of freedom in solution are treated as they are in the gas phase, the cost associated with their loss when two or more molecules form a complex system in solution is overestimated, and consequently, these processes are kinetically overpenalized in solution, leading to rate constants that are artificially underestimated.

The presence of a nonpolar solvent, benzene in the present study, was found to increase the feasibility of all of the studied reactions, i.e., to lower the height of the barrier (Table 3). In the gas phase, only the reactions with hydroxyl and methyl radicals were found to be exergonic ( $\Delta G < 0$ ), whereas in solution, the reactions with methoxyl and formyl radicals also become exergonic. As expected, the largest free energy release was obtained for the OH radical, which is the most reactive, and consequently the most dangerous, of the free radicals studied. It should be noticed that, for CH<sub>3</sub>O, the endergonicity is very small and might easily be overcome at higher temperatures.

The rate constants (k) per addition site at 298.15 K are also reported in Table 3. They were first calculated using the conventional transition-state theory (TST) as

$$k = \frac{k_{\rm B}T}{h} \,\mathrm{e}^{-(\Delta G^{\ddagger})/RT} \tag{2}$$

where  $k_{\rm B}$  and h are the Boltzmann and Planck constants, respectively, and  $\Delta G^{\dagger}$  is the Gibbs free energy of activation. However, some of the k values calculated in this way are near or even higher than the diffusion-limited rate constant. Accordingly, the apparent rate constant ( $k_{\rm app}$ ) cannot be directly obtained from TST calculations. In the present work, we used Collins–Kimball theory for that purpose<sup>26</sup>

$$k_{\rm app} = \frac{k_{\rm D} k_{\rm act}}{k_{\rm D} + k_{\rm act}} \tag{3}$$

where  $k_{\rm act}$  is the activation rate constant (obtained from TST calculations, eq 2) and  $k_{\rm D}$  is the diffusion-controlled rate constant ( $k_{\rm D} \approx 1 \times 10^{10} \ {\rm L \ mol^{-1} \ s^{-1}}$ ).

As the values in Table 3 show, with the exception of the reactions involving the OOH and CH<sub>3</sub>OO radicals, the rate constants per addition site remain very close to the diffusion limit, supporting the hypothesis that carbon nanotubes are expected to act very efficiently as free-radical scavengers.

It should be noticed that, once a free radical is attached to the CNT structure, the latter becomes a free radical itself. Such a CNT radical is expected to be much less reactive than the original radical but more reactive than the original pristine CNT. Therefore, the addition of a second radical should be energetically more favored. Accordingly, for the reaction of the (5,5) CNT fragment with OH, further additions of up to four OH radicals were also modeled. For the addition of a second radical, four different reaction sites were considered (Figure 1), with the two OH groups bonded to carbon atoms that are next to each other (I), separated by one C atom (II), separated by two C atoms (III), and opposite each other (IV). As the geometries in Figure 1 show, when the second OH is in the vicinity of the first, the two groups are oriented in such a way that the H atom in one of them is pointing toward the O atom in the other, leading to an intramolecular interaction. The distance between these atoms was found to be 1.73 and 2.31 Å for isomers I and II, respectively. For isomers III and IV, on the other hand, the two hydroxyl groups are too far apart to allow this kind of interaction, and the H atoms in the OH groups are pointing toward the center of a ring, probably due to a H  $\cdots$   $\pi$  interaction as has previously been described for other aromatic compounds. The presence of these interactions is expected to lower the energy of the adducts, at least in the gas phase, and it is also expected that a stronger interaction will result in a lower energy for the adduct. As a result, the geometrical features suggest that adduct I should have the lowest energy of all of the modeled

The enthalpies of reaction and the Gibbs free energies of reaction for the additions of a second OH radical are reported in Table 4; they were calculated taking the product of the first addition as the reactant. All of the second OH additions were found to be exothermic and exergonic (Table 4). Adduct II is predicted to be least likely to form in both the gas phase and nonpolar solution, with an energy at least 10 kcal/mol higher than those of any other of its isomers. This finding can be justified based on the fact that hydroxyl groups orient electrophilic attacks at ortho and para positions, whereas in isomer II, the second OH is at a meta position with respect to the first. Thus, it seems that there are two factors governing the relative stability of the isomers with two hydroxyl groups on the CNT: the ortho/para directing character of the OH group already attached to the surface and the H-bond interactions between OH groups. Both factors favor the formation of isomers I and III, whereas H bonding is not possible in isomer IV, and isomer II does not conform with the directing character of the OH group.

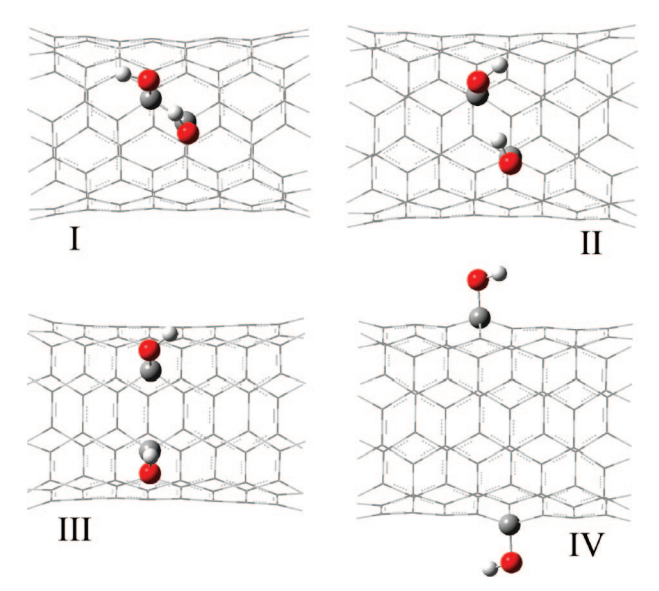


**Figure 1.** Optimized geometries of modeled products for the addition of a second OH radical to the (5,5) CNT fragment.

TABLE 4: Gibbs Free Energies of Reaction ( $\Delta G$ ) and Enthalpies of Reaction ( $\Delta H$ ) at 298.15 K for the Additions of Two to Four Hydroxyl Radicals to a (5,5) CNT Fragment

	$\Delta H_{\rm gas}$ (kcal/mol)	$\Delta H_{\rm sol}$ (kcal/mol)	$\Delta G_{ m gas}$ (kcal/mol)	$\Delta G_{ m sol}^{ m FV}$ (kcal/mol)		
Two OH						
I	-38.41	-39.50	-27.18	-32.70		
II	-16.46	-16.65	-5.09	-9.71		
III	-33.31	-39.25	-22.55	-32.92		
IV	-26.82	-26.27	-15.56	-19.44		
Three OH						
$\mathbf{V}$	-46.18	-44.47	-34.11	-36.83		
VI	-23.64	-23.30	-12.69	-16.78		
VII	-35.92	-37.63	-24.95	-31.09		
Four OH						
IX	-59.24	-58.80	-46.83	-50.81		
X	-43.61	-43.26	-31.38	-35.46		

Adduct I is expected to be the most abundant structure in the gas phase, whereas in nonpolar solutions, it is expected to be formed to about the same extent as adduct III. The presence of the solvent was found to lower the Gibbs free energies of reaction compared to the values in the gas phase. The most probable second OH additions were found to be significantly more exergonic than the first OH additions, supporting an increase in the reactivity from CNT to CNT—OH.

The energies of the third OH addition process were computed taking isomer I as the reactant. Three different products were modeled in this case (Figure 2). All of the third OH additions were found to be exothermic and exergonic. Isomer V is predicted to be the lowest in energy and, therefore, the most abundant. The lower energy of isomer V compared to isomers VI and VII seems to be caused by H-bond interactions involving the hydroxyl groups: these interactions are expected to be stronger in isomer V. The orders in enthalpy and Gibbs free energy of reaction for the studied channels were found to be the same in the gas phase and in solution: V > VII > VI. The  $\Delta H$  and  $\Delta G$ values for the formation of adduct V are more negative than those for the formation of adduct I, suggesting that CNT-2OH has a higher reactivity than CNT-1OH, despite of the fact that the latter is a radical species. Thus, it can be inferred that OH-OH interactions contribute more significantly to relative

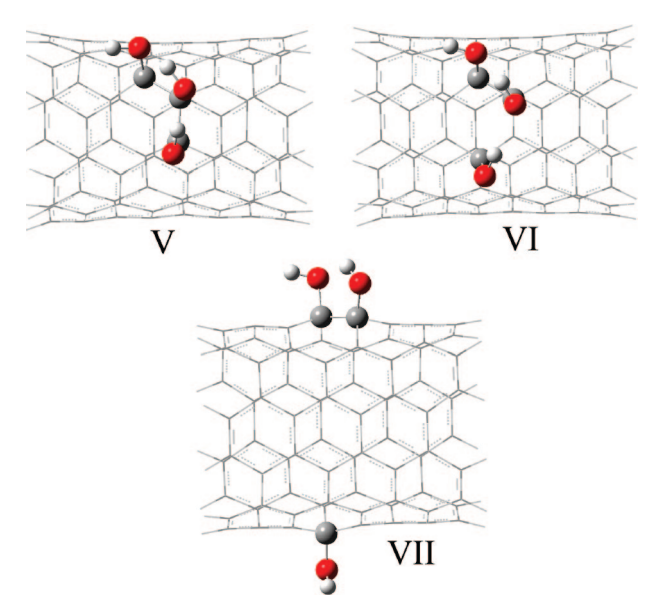


Figure 2. Optimized geometries of modeled products for the addition of a third OH radical to the (5,5) CNT fragment.

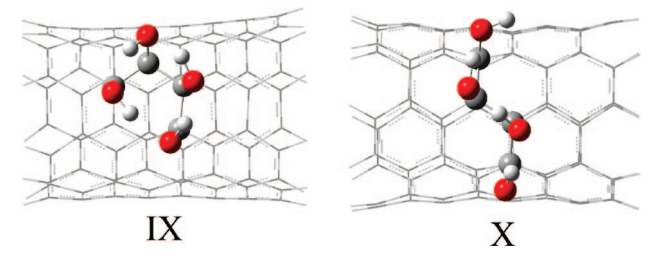


Figure 3. Optimized geometries of modeled products for the addition of a fourth OH radical to the (5,5) CNT fragment.

binding energies than pairing of spins for even numbers of attached hydroxyl groups.

The addition of a fourth OH to isomer V was also computed, and two different products of reaction were considered. Both of the modeled products had all of the OHbonded atoms placed consecutively in the carbon network (Figure 3), one with all of the OH groups in the same hexagon (IX) and the other with the fourth OH in a different hexagon. The possibility of the new OH radical adding to a C atom at the opposite side of the nanotube was not included this time because, for all of the previously discussed cases, such a possibility was never the most energetically favored one. As the values in Table 4 show, the fourth OH additions are exothermic and exergonic to a larger extent than the third OH additions. Isomer IX is predicted to be 15.5 and 14.7 kcal/mol lower than isomer **X**, in terms of enthalpy and Gibs free energy, respectively. This seems to be caused by the OH-OH hydrogenbond interactions, because there are four such interactions in isomer IX and three in isomer X.

Gathering all of the previously discussed results, some generalizations can be made. Once a first radical is attached to a CNT, the further additions are increasingly feasible, suggesting that CNTs can act as free-radical sponges. For reactions with OH radicals, at least for armchair nanotubes, subsequent additions are expected to lead to products in which the OH groups are distributed in clusters rather than evenly spread on the nanotubes.

It remains an open question whether the chirality and curvature of the nanotubes might influence their efficiency as free-radical traps. However, comparing the results from this

**TABLE 5:** Global Reactivity Indexes Hardness  $(\eta)$ , Electrophilicity ( $\alpha$ ), and Electrophilicity ( $\omega$ ) for Nonradical **Species** 

	gas phase		solution			
	η (eV)	χ (eV)	ω (eV)	η (eV)	χ (eV)	ω (eV)
CNT	0.896	3.421	6.528	0.839	3.427	6.997
I	0.426	3.637	15.512	0.424	3.661	15.813
II	0.477	3.748	14.723	0.483	3.769	14.708
III	0.620	3.590	10.402	0.618	3.612	10.556
IV	0.421	3.728	16.506	0.426	3.747	16.474
$\mathbf{IX}$	0.984	3.593	6.558	0.983	3.610	6.629
$\mathbf{X}$	1.087	3.582	5.903	1.096	3.608	5.942

work ( $\Delta H_{\text{gas}}$ , Table 2) with those previously reported for the graphite + OH reaction, 11,12 it seems that the curvature of the nanotube increases the feasibility of the process. The energy evolved upon the addition of one OH radical to a CNT was found to be about -26 kcal/mol, whereas it was reported to be much lower for OH addition to graphite: only about  $-5^{12}$  or  $-12^{11}$  kcal/mol.

The nonradical nanotubes, i.e., those with zero or an even number of OH groups attached, are stable species that can be used for other purposes. Accordingly, the properties of these compounds were analyzed in terms of four global reactivity indexes, namely, hardness  $(\eta)$ , electronegativity  $(\chi)$ , chemical potential  $(\mu)$ , and electrophilicity  $(\omega)$ , as well as density of states (DOS) calculations.

The absolute hardness was quantified by Parr and Pearson as the second derivative of the electronic energy of the system with respect to the number of electrons at a constant external potential<sup>27</sup>

$$\eta = \frac{1}{2} \left( \frac{\partial^2 E}{\partial N^2} \right)_{y(r)} \tag{4}$$

The hardness evaluations were all based on the commonly used finite difference approximation, leading to

$$\eta = \frac{I - A}{2} \tag{5}$$

where *I* and *A* represent the ionization potential and the electron affinity, respectively. According to Koopmans' theorem,<sup>28</sup> eq 5 becomes

$$\eta = \frac{-(\epsilon_{\text{HOMO}} - \epsilon_{\text{LUMO}})}{2} = \frac{\epsilon_{\text{LUMO}} - \epsilon_{\text{HOMO}}}{2} \tag{6}$$

where  $\in_{LUMO}$  and  $\in_{HOMO}$  are Kohn-Sham one-electron eigenvalues associated with the lowest unoccupied molecular orbital (LUMO) and the highest occupied molecular orbital (HOMO), respectively, obtained from DFT calculations on the neutral

The chemical hardness generally measures the resistance of a system to change in the electron number or the shape of the electron cloud. Thus, it can be used as a global reactivity index to predict reactivity in the context of charge-transfer processes. An increase in  $\eta$  implies a more stable, i.e., less reactive, system. The results in Table 5 show that the systems with two hydroxyl groups have lower hardness values than pristine CNTs, whereas those with four OH groups have higher  $\eta$  values than pristine nanotubes.

The chemical potential  $(\mu)$  is defined as the partial derivative of the system's energy (E) with respect to the number of electrons (N) at a fixed external potential  $v(r)^{27}$ 

$$\mu = \left(\frac{\partial E}{\partial N}\right)_{\nu(r)} \tag{7}$$

The chemical potential is the negative of the electronegativity  $(\chi)$  concept of Pauling and Mulliken,<sup>29</sup> which can be calculated as

$$\chi = \frac{I+A}{2} = -\mu \tag{8}$$

Applying Koopmans' theorem<sup>28</sup> to eq 8, one obtains

$$\chi = -\frac{\epsilon_{\text{HOMO}} + \epsilon_{\text{LUMO}}}{2} \tag{9}$$

Differences in  $\chi$  drive electron transfer. Electrons tend to flow from a region of low electronegativity to a region of high electronegativity, and the number of electrons flowing is linearly proportional to the difference in  $\chi$ . According to values in Table 4, the presence of OH groups in the CNT structures increases their electronegativity, both in the gas phase and in nonpolar solutions, which is consistent with the nature of OH groups.

Additionally, electrophilicity descriptors were also calculated  $as^{30}\,$ 

$$\omega = \frac{\mu^2}{2\eta} \tag{10}$$

This index measures the stabilization in energy when the system acquires an additional electronic charge from the environment, i.e., the propensity of a species to "soak up" electrons. By definition, it encompasses both the ability of an electrophile to acquire additional electronic charge and the resistance of the system to exchange electronic charge with the environment. The largest values of  $\chi$  were found for CNTs with two hydroxyl groups, and the lowest were found for those with four OH groups attached.

The nature of the nanotube electronic density of states (DOS) near the Fermi level  $(E_f)$  is critical to the understanding of electrical transport through these materials. Isolated armchair nanotubes are metallic with a finite DOS at  $E_{\rm f}$ . For "infinite" nanotubes, i.e., those with a diameter (D) that is much smaller than their length (L), van Hove singularities, which reflect the one-dimensional (1D) band structure of the nanotubes and appear as sharp peaks in the DOS, are expected. Structural modifications of nanotubes also have an effect on their DOS spectrum.<sup>31</sup> Accordingly, the DOS of the pristine nanotube (CNT) and those for structures with two and four OH groups per fragment (I and IX, respectively) are compared in Figure 4. The shape of the DOS also depends on the model used to represent the SCWNTs. When the nanotubes are modeled as finite fragments, where the condition  $D \ll L$  does not apply, a band gap appears. Accordingly, in addition to the finite models previously described, the nanotubes were also modeled as 1D periodic systems for DOS calculations. In this case, the unit cell was chosen from the optimized fragments by removing the H atom and one C ring at each end of the fragments.

For the finite fragments (Figure 4A), there is a gap around the Fermi level for the pristine nanotube. The presence of two hydroxyl groups in the structure (I) significantly reduces the magnitude of the gap, whereas for the structure with four OH groups (IX), the gap is similar to that of the pristine nanotube. When the nanotubes are modeled as 1D periodic systems (Figure 4B), there is a finite electron density at the Fermi level for the pristine nanotube, and the van Hove singularities are clearly observed. When there are OH groups on the nanotube structures, the sharp peaks in the DOS disappear, probably because of the rupture of the  $\pi$  conjugation and the break in symmetry.

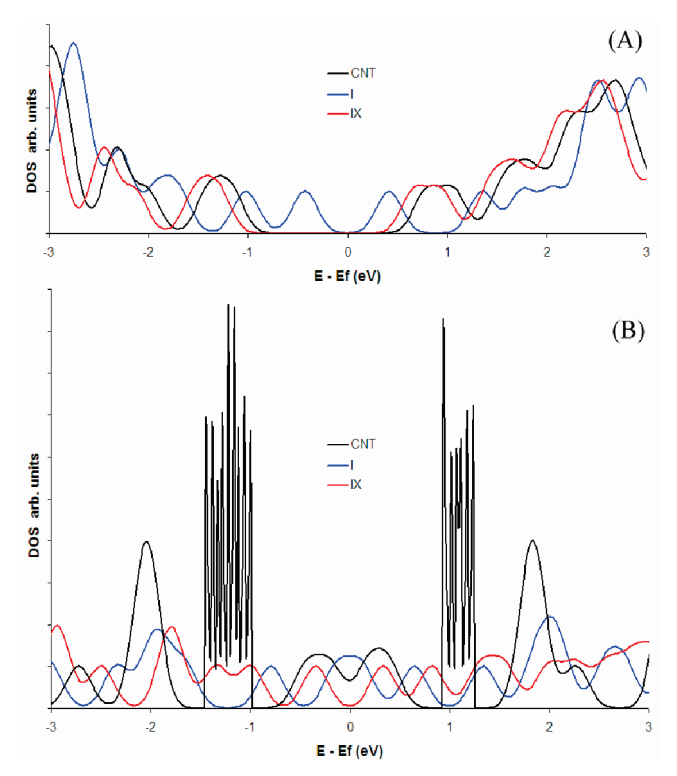


**Figure 4.** Qualitative picture of the total electron density of states (DOS) with the zero of energy axis set at the Fermi level: (A) molecular fragment, (B) periodic system.

Compared to the pristine nanotube, there is an increase in the electronic density at  $E_{\rm f}$  for structure **I**, whereas for structure **IX**, there is a significant DOS decrease at  $E_{\rm f}$ . In the latter case, almost a pseudo-gap is present, and the metallic behavior is expected to be affected.

In general, according to the reactivity indexes and DOS previously discussed, it can be suggested that, by controlling the proportion of OH groups on the nanotubes, their properties can be manipulated.

### Conclusions

The potential ability of single-walled carbon nanotubes to act as free-radical scavengers has been studied using density functional theory calculations. For that purpose, the reactions of a (5,5) SWCNT fragment with six different radicals were studied, and for hydroxyl radical, which is the most reactive and dangerous of the radicals considered, up to four additions were modeled.

All of the studied reactions were found to be exothermic. They also were found to be exergonic, except those involving OOH and CH<sub>3</sub>OO radicals, which are slightly endergonic. The presence of nonpolar environments seems to enhance the reactivity of SWCNT fragments toward free radicals, compared to the gas phase.

Once a first radical is attached to the nanotube, further additions are increasingly feasible, suggesting that SWCNTs can act as free-radical sponges.

For reactions with OH radicals, subsequent additions are expected to lead to products in which the OH groups are distributed in clusters rather than regularly spread in the nanotube.

Because stable (nonradical) OH-modified SWCNTs can be used for other purposes, their properties were analyzed in terms of global reactivity indexes and density of states (DOS). The

results from these analyses suggest that, by controlling the proportion of OH on the nanotubes, their properties can be manipulated.

**Acknowledgment.** The author gratefully acknowledges the financial support from the Instituto Mexicano del Petróleo (IMP) through Project D00446 and thanks the IMP Computing Center for supercomputer time on SGI Origin 3000.

#### **References and Notes**

- (1) (a) Iijima, S. *Nature* **1991**, *354*, 56. (b) Bethune, D. S.; Kiang, C. H.; deVries, M. S.; Goreman, G.; Savoy, R.; Vazquez, J.; Beyers, R. *Nature* **1993**, *363*, 605.
- (2) See, for example:(a) Rinzler, A. G.; Hafner, J. H.; Nikolaev, P.; Lou, L.; Kim, S. G.; Tomanek, D.; Nordlander, P.; Colbert, D. T.; Smalley, R. E. Science 1995, 269, 1550. (b) de Heer, W. A.; Chatelain, A.; Ugarte, D. Science 1995, 270, 1179. (c) Treacy, M. M. J.; Ebbesen, T. W.; Gibson, J. M. Nature 1996, 381, 678.
- (3) Dubois, D.; Kadish, K. M.; Flanagan, S.; Wilson, L. J. J. Am. Chem Soc. 1991, 113, 7773.
- (4) Xie, Q. S.; Perezcordero, E.; Echegoyen, L. J. Am. Chem. Soc. 1992, 114, 3978.
  - (5) Krinsky, N. I. Annu. Rev. Nutr. 1993, 13, 561.
- (6) Edge, R.; McGarvey, D. J.; Truscott, T. G. *J. Photochem. Photobiol.* **1997**, *41*, 189.
- (7) Fenoglio, I.; Tomatis, M.; Lison, D.; Muller, J.; Fonseca, A.; Nagy, J. B.; Fubini, B. Free Radical Biol. Med. 2006, 40, 1227.
- (8) Morton, J. R.; Preston, K. F.; Krusic, P. J.; Hill, S. A.; Wasserman, E. J. Phys. Chem. **1992**, *96*, 3576.
- (9) Borghi, R.; Lunazzi, L.; Placucci, G.; Krusic, P. J.; Dixon, D. A.; Matsuzawa, N.; Ata, M. J. Am. Chem. Soc. 1996, 118, 7608.
- (10) Gan, L.; Huang, S.; Zhang, X.; Zhang, A.; Cheng, B.; Cheng, H. J. Am. Chem. Soc. 2002, 124, 13384.
- (11) Jelea, A.; Marinelli, F.; Ferro, Y.; Allouche, A.; Brosset, C. Carbon **2004**, *42*, 3189.
- (12) Xu, S. C.; Irle, S.; Musaev, D. G.; Lin, M. C. J. Phys. Chem. A 2007, 111, 1355.
  - (13) Kong, H.; Gao, C.; Yan, D. J. Am. Chem. Soc. 2004, 126, 412.
- (14) Koch, W.; Holthaussen, M. C. A Chemist's Guide to Density Functional Theory; Wiley-VCH: Weinheim, Germany, 2000.
- (15) Parr, R. G.; Yang, W.; Density-Functional Theory of Atoms and Molecules, Oxford University Press: New York, 1989.
- (16) Frisch, M. J.; Trucks, G. W.; Schlegel, H. B.; Scuseria, G. E.; Robb, M. A.; Cheeseman, J. R.; Montgomery, J. A., Jr.; Vreven, T.; Kudin, K. N.; Burant, J. C.; Millam, J. M.; Iyengar, S. S.; Tomasi, J.; Barone, V.; Mennucci, B.; Cossi, M.; Scalmani, G.; Rega, N.; Petersson, G. A.;

- Nakatsuji, H.; Hada, M.; Ehara, M.; Toyota, K.; Fukuda, R.; Hasegawa, J.; Ishida, M.; Nakajima, T.; Honda, Y.; Kitao, O.; Nakai, H.; Klene, M.; Li, X.; Knox, J. E.; Hratchian, H. P.; Cross, J. B.; Bakken, V.; Adamo, C.; Jaramillo, J.; Gomperts, R.; Stratmann, R. E.; Yazyev, O.; Austin, A. J.; Cammi, R.; Pomelli, C.; Ochterski, J. W.; Ayala, P. Y.; Morokuma, K.; Voth, G. A.; Salvador, P.; Dannenberg, J. J.; Zakrzewski, V. G.; Dapprich, S.; Daniels, A. D.; Strain, M. C.; Farkas, O.; Malick, D. K.; Rabuck, A. D.; Raghavachari, K.; Foresman, J. B.; Ortiz, J. V.; Cui, Q.; Baboul, A. G.; Clifford, S.; Cioslowski, J.; Stefanov, B. B.; Liu, G.; Liashenko, A.; Piskorz, P.; Komaromi, I.; Martin, R. L.; Fox, D. J.; Keith, T.; Al-Laham, M. A.; Peng, C. Y.; Nanayakkara, A.; Challacombe, M.; Gill, P. M. W.; Johnson, B.; Chen, W.; Wong, M. W.; Gonzalez, C.; and Pople, J. A. *Gaussian 03*, revision D.01; Gaussian, Inc.: Wallingford, CT, 2004.
- (17) Dennington, R., II; Keith, T.; Millam, J.; Eppinnett, K.; Hovell, W. L.; Gilliland, R. *GaussView*, version 2.0; Semichem, Inc.: Shawnee Mission, KS, 2003.
- (18) (a) Cances, M. T.; Mennucci, B.; Tomasi, J. J. Chem. Phys. 1997, 107, 3032. (b) Mennucci, B.; Tomasi, J. J. Chem. Phys. 1997, 106, 5151. (c) Mennucci, B.; Cances, E.; Tomasi, J. J. Phys. Chem. B 1997, 101, 10506. (d) Tomasi, J.; Mennucci, B.; Cances, E. J. Mol. Struct. (THEOCHEM) 1999, 464, 211.
- (19) Curtiss, L. A.; Raghavachari, K.; Redfern, P. C.; Pople, J. A. J. Chem. Phys. 1997, 106, 1063.
- (20) Curtiss, L. A.; Redfern, P. C.; Raghavachari, K.; Pople, J. A. J. Chem. Phys. 1998, 109, 42.
- (21) Curtiss, L. A.; Raghavachari, K.; Redfern, P. C.; Rassolov, V.; Pople, J. A. *J. Chem. Phys.* **2000**, *112*, 7374.
  - (22) Okuno, Y. Chem.-Eur. J. 1997, 3, 212.
- (23) Benson, S.W. *The Foundations of Chemical Kinetics*; Krieger: Malabar, FL, 1982.
- (24) Ardura, D.; Lopez, R.; Sordo, T. L. J. Phys. Chem. B 2005, 109, 23618.
- (25) (a) Alvarez-Idaboy, J. R.; Reyes, L.; Cruz, J. *Org. Lett.* **2006**, 8, 1763. (b) Galano, A. *J. Phys. Chem. A* **2007**, *111*, 1677 Addition/Correction: Galano, A. *J. Phys. Chem. A* **2007**, *111*, 4726. (c) Alvarez-Idaboy, J. R.; Reyes, L.; Mora-Diez, N. *Org. Biomol. Chem.* **2007**, 3682. (d) Galano, A.; Cruz-Torres, A. *Org. Biomol. Chem.* **2008**, 6, 732.
  - (26) Collins, F.C.; Kimball, G.E. J. Colloid Sci. 1949, 4, 425
  - (27) Parr, R. G.; Pearson, R. G. J. Am. Chem. Soc. 1983, 105, 7512.
  - (28) Koopmans, T. Physica 1933, 1, 104.
- (29) Parr, R. G.; Donnelly, R. A.; Levy, M.; Palke, W. E. *J. Chem. Phys.* **1978**, *68*, 3801.
- (30) Parr, R. G.; Szentpaly, L.; Liu, S. J. Am. Chem. Soc. 1999, 121, 1922
- (31) See, for example:(a) Galano, A.; Orgaz, E. *Phys. Rev. B* **2008**, *77*, 045111. (b) Park, K. A.; Choi, Y. S.; Lee, Y. H. *Phys. Rev. B* **2003**, *68*, 045429. (c) Mavrandonakis, A.; Froudakis, G. E. *Nano Lett.* **2003**, *3*, 1481.

JP801379G